Journal of Petroleum Exploration and Production Technology (2023) 13:803–812
https://doi.org/10.1007/s13202-022-01576-0

ORIGINAL PAPER - EXPLORATION ENGINEERING

Application of digital rock technology for formation damage evaluation in tight sandstone reservoir

Zhao Xiong[1] · Guanqun Wang[1] · Yuguang Zhang[2] · Haoran Cheng[1,3] · Feifei Chen[1] · Wei Long[1,3]

Received: 29 December 2021 / Accepted: 17 October 2022 / Published online: 26 October 2022

Abstract
Formation damage is a common phenomenon and is impaired to the reservoir by reducing the productivity. Formation damage is usually caused by solids plugging, clay swelling, saturation changes, etc., and fracturing fluids with a series of chemical additives are pumped into the well for production enhancement. It is difficult to optimize the fracture fluids and well shut-in time due to lack of fundamental understandings. Currently, little research has been done to investigate the mechanisms of formation damage at the pore scale. In this study, a combination of digital rock technology and core sample laboratory soaking experiments is used to evaluate the formation damages for different fracture fluids in tight sandstone reservoir. Three core samples from a full-diameter core are soaked in three different fracture fluids (surfactant, polymer, and gel) for eight different durations (from 2 h to 15d) to simulate well shut-in process. The samples in various soak times are scanned by X-ray micro-computer tomography (Micro-CT) to obtain the 3D images of the true geometry. The images are then compared to optimize the fracture fluids and quantify the damage degree after various well shut-in times. Then, displacement processes are simulated using lattice Boltzmann method (LBM) to evaluate the residual oil saturations and optimize the well shut-in time. The study suggests that the well shut-in process can cause irreversible damage to tight sandstone reservoir even for optimized fracture fluid. In the initial shut-in stages, clays swelling dominates pore structure alteration and reduces the porosity. Calcite will dissolute after which lead to slight porosity increase. In the flowback process after well shut-in, the simulated residual oil saturation will decrease initially and then increase after, which is complied with the porosity variation. The digital rock technology combined with the soaking experiments will provide alternative method for the evaluation of formation damage and the optimization of well shut-in time in tight sandstone reservoir, which can guide the selection of the fracture fluids and onsite fracturing operation.

Keywords Fracture fluid · Formation damage evaluation · Digital rock · Tight sandstone · Shut-in time

Introduction

In recent years, unconventional resources have gained popularity increasingly. Stimulation with the fracturing fluids is the main means for the effective development and production of tight reservoirs. Since the fracturing fluid will enter the matrix and have reactions with the mineral, the rock and fluid contact time will directly affect the stimulation effect. Thus, the formation damage evaluation and shut-in time optimization are crucial.

The conventional method for formation evaluation of fracturing fluid is to compare the permeability before and after the fluid invasions (Liang et al. 2017; Rui et al. 2018; You et al. 2019). And large-scale physical simulation experiment and macroscopic-scale numerical simulation are combined to obtain optimal well shut-in time (Izgec 2009; Li et al. 2011; Cense et al. 2011; Vocke 2018; Wang et al. 2020). However, the conventional laboratory techniques to determine the physical properties (such as porosity, mercury injection, and relative permeability) are usually based on perfectly cylindrical core plugs or large amounts of crushed-rock materials (Mcphee et al. 2015). The high-quality core requirements and usually destructive experiment will invisibly increase the time and the cost for conventional

✉ Wei Long
wei.long@icore-group.com

1 ICORE GROUP INC, Shenzhen 518057, China

2 CNPC, Daqing 163458, China

3 Research Institute of Tsinghua University, Shenzhen, Shenzhen 518057, China

laboratory experiments, especially for tight reservoirs (Wang et al. 2016; Xie et al. 2017). Also, the poor petrophysical properties make it difficult to exploit the unconventional resources by conventional laboratory methods. These problems have promoted the oil and gas industry to search for more advanced technologies.

The digital rock (DR) technology, combined with X-ray computed tomography (CT) and direct numerical simulation (DNS) based on the scanned 3D geometry images, has drawn interests of scholars in recent years, due to their advantages in visualization and time effective for predicting the physical properties (Rassenfoss 2011; Walls 2012; Fredrich 2014; Mukherjee 2016; Jerauld 2017). DR analysis has been performed to simulate the routine core analysis (RCA) such as porosity and permeability, as well as special core analysis (SCAL) such as capillary pressure, relative permeability, and electrical properties. (Zhao et al. 2010; Singh et al. 2011; Sun et al. 2017, 2019). Pore-scale digital rock data could provide direct information of the pore geometry and pore throat distribution, which will improve the understanding of the reservoir characterization and enhance the reservoir performance and hydrocarbon recovery (Mclendon et al. 2014; Andrew et al. 2014; Guo et al. 2018).

In this study, we combine the laboratory soaking experiments with DR technology to evaluate the formation damages for various fracture fluids in tight reservoir for Daqing oilfield, Northeastern China. Three core samples from a full-diameter core are soaked in three different fracture fluids (surfactant, polymer, and gel) for eight different durations (from 2 h to 15d). The samples after various soak times are scanned by micro-CT to obtain the true 3D geometry. The images are compared to optimize the fracture fluid and quantify the damage degree after various well shut-in times. Then, the displacement processes are simulated using lattice Boltzmann method (LBM) to evaluate the residual oil saturations and optimize the well shut-in time. This method will provide alternatives for formation damage evaluation and guide onsite fracturing operation in tight sandstone reservoir.

Methods

Laboratory experimental design

Six micro-core samples with a physical size of 10–20 mm^3 are drilled from two full-diameter cores of two wells (three samples each well) located in Daqing Oilfield, Northeastern China. Laboratory experiments are carried out as follows: (1) The samples are divided into two groups according to their well numbers (A and B) and scanned by micro-CT to generate the true 3D geometries. The calculated average porosity and permeability are 5.56%, 0.84mD and 2.28%, 0.43mD, for well A and B, respectively. (2) Three samples in each group are soaked in three different fracture fluids, that is, surfactant, gel and polymer, under reservoir conditions (20 MPa, 194 K) for eight different durations (2 h, 6 h, 12 h, 1 day, 2 days, 3 days, 7 days, and 15 days). After each soaking time, the samples are then taken out for micro-CT scanning with a resolution of 0.5 μm. (3) The scanned images are compared with the images of the original cores to visualize and quantify the alterations in pore structures. Porosity reduction is calculated to quantify the formation damage degrees for different soaking durations, and the fracture fluid for such formation can be then optimized. (4) The 3D pore structures of different soaking durations will be used for multiphase flow simulation to mimic the flowback production process and optimize the well shut-in time.

The micro-CT used in this study is nanoVoxel-3502E, manufactured by Sanying in China. The view field of the equipment is the industry's top 1920 × 1920 × 1920 grid. And the scanner is equipped with a microfocus ray source up to 300 kV, which ensures the high-precision detection capability. There are a ray source on one side and a signal receiver on the other side (Fig. 1). The samples are fixed on the middle turntable and rotate at low speed. Hundreds of sample images were taken from different angles, and then, image reconstruction is carried out to obtain the three-dimensional structures. The limit of the scanning resolution is 0.5 μm.

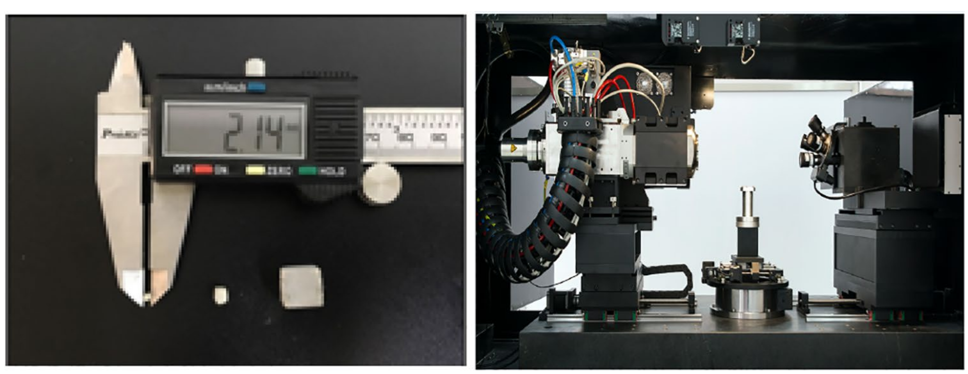

(a) Micro-core sample (b) Internal structure of micro-CT

Fig. 1 Samples and internal structure of micro-CT

Table 1 Mineral contents of samples

Samples	Mineral contents, %				Clay contents, %
	Quartz	Potassium feldspar	Plagioclase	Calcite	
Well A	35.9	0.9	16.1	33.5	13.6
Well B	45.3	1.0	22.1	9.0	22.6

Core sample, fracture fluids information

Table 1 lists the mineral contents of the full-diameter core, and Table 2 shows the contents of clay minerals. The contents of clay minerals of the two wells are very similar. However, the calcite content of well B is much smaller than that of well A.

Table 3 gives the detailed compositions of the three different fracture fluids in this study that are also widely used in the oilfield. Recently, environmentally friendly chemicals attract more attentions and the green IOR/EOR agents are investigated by a lot of researchers (Bing et al. 2018; Nasiru et al. 2020).

Image segmentation method

After high-resolution micro-CT scanning, the 3D images will be analyzed and segmented into pores and rock skeletons to build the 3D model. A trainable segmentation software was independently developed to improve the segmentation efficiency and accuracy. The machine learning algorithm which uses the same fundamentals as WEKA was used for image segmentation in this study (Arganda-Carreras et al. 2017). Two or more images will be manually selected as input images for training. The accuracy of the segmentation depends on the amount of the trained images. More trained images also mean longer calculating time and requirement for more powerful computing resources. It has been described in previous papers that the accuracy of any segmentation method cannot be taken for granted without rigorous validation because different segmentation methods may yield different levels of uncertainty even for a relatively simple sandstone (Blunt et al. 2012; Sun et al. 2017). The porosity resulting from segmentation by machine learning should be compared to that of laboratory experiment. As shown in Fig. 2a, the areas that are marked by green lines are typical rock skeleton, while the red line areas are typical pores. These marked areas acted as input information for training. Figure 2b is the segmented results by machine learning method. The porosity of the segmented 3D structure for sandstone (12.0%) is comparable with the laboratory measurement (12.5%).

Flow simulation method

LBM has attracted interest of researchers in oil and gas industry (Cancelliere et al. 1990; Martys and Chen 1996). LBM is a computational fluid dynamics approach based on the kinetic theory of gas. It can solve discrete velocity Boltzmann equation (DVBE). According to the classical asymptotic analysis of Chapman–Enskog (CE) expansion, the DVBE approximates a series of fluid dynamics equations including incompressible Navier–Stokes (NS) equation. The first-order CE expansion of the DVBE approximates the incompressible NS equation with a remainder up to third order of the Mach number. Therefore, LBM is effective for low-speed incompressible flow, especially for flow in porous media with irregular geometries (Shan and Doolen 1995; Kang et al. 2002; Pan et al. 2004). We used Shan-Chen multi-component multiphase flow model in this study to simulate two-phase flow. The previous work has been done using the LBM in other applications (Yang et al. 2021a, b; Yang et al. 2021a, b). In this study, CT images

Table 2 Contents of clay minerals

Samples	Clay mineral content, %						S, %	
	Smectite	I/S	Illite	Kaolinite	Chlorite	C/S	I/S	C/S
Well A	/	51	13	5	31	/	10	/
Well B	/	52	10	3	35	/	10	/

Table 3 Fracture fluid composition

Composition	Base fluid	Crosslinker	Crosslink ratio	Gel breaker
Surfactant	2%Surfactant	30%KCL	40:1	Dilute 10 times
Polymer	0.25%Polymer + 0.4%Additives	40%Crosslinker	50:1	0.05% $K_2S_2O_8$
Gel	0.45%Gel + 0.06%Na_2CO_3 + 0.02%$NaHCO_3$ + 0.4%additives + 0.08%Defoamer	4%GW150 + 7%DW90	50:1	0.05% $K_2S_2O_8$

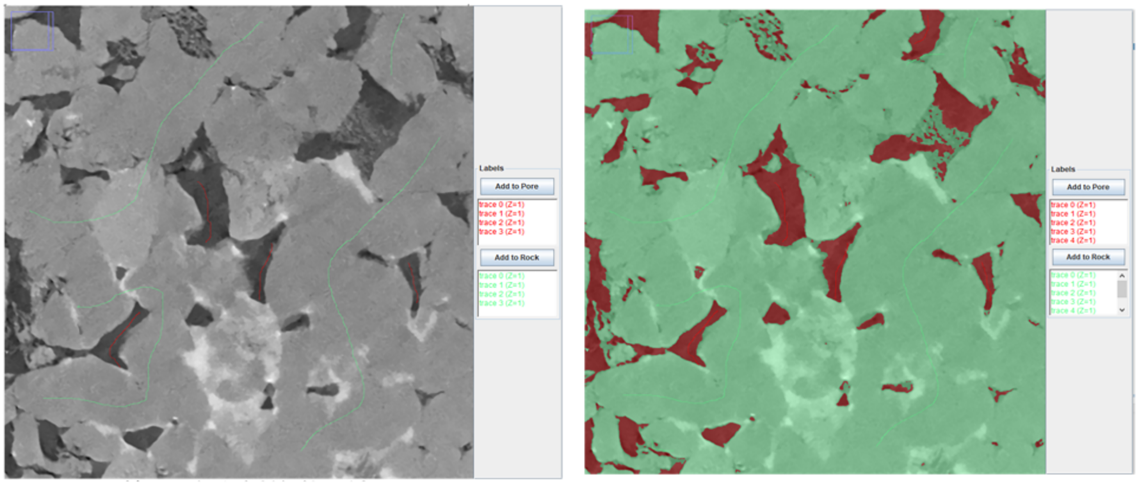

a) gray image b) binary image

Fig. 2 Images before and after segmentation by machine learning method

are used for LBM simulation to investigate the residual oil saturation at various soaking times. Water displacing oil is simulated with a size of 400^3 to mimic the flowback process. The inlet density is set to be 1.0/0.01, and outlet density of 0.01/0.8 for water and oil, respectively. Thus, pressure differential leads to two-phase flow with a capillary number of 10^{-5}. We set the viscosity of water and oil equally where $\tau_w = \tau_o = 1$.

Results and analysis

Formation damage evaluation

Figure 3 shows the original gray images of core samples from well A soaking in different fracture fluids for different durations. Since the principle of CT imaging technology is based on the different absorption degrees of X-ray by substances with different densities, the lower the density is, the darker the color. Thus, the black represents pores or fluids, white represents calcite, and gray represents the grains as shown in Fig. 3. Various fluids are filled within the pore (shown in black), respectively.

In Fig. 3a, the pore throat size has been increased slightly during the 2 hours' soaking in the surfactant, and the grain's contact surface has already been dissolved after 7 day (red lines). In Fig. 3b, the pores in marginal area show a little increase after 2-h's soaking in the polymer. Then, pore amplifying pushes toward the core center and calcite in marginal area is dissolved after 3 day (red circle). In the 7th day, nearly half of the calcites are dissolved and the whole structure is almost destroyed. In Fig. 3c, there is a negligible pore structure change after 2 h, 3 days and 7 days soaking in the gel. Figure 4 shows the calculated calcite percentage through CT images after various soaking time for different fluids, which clearly shows the calcite dissolution for polymer and negligible impact for gel.

Since the rock skeleton dispersion and particles transport in later production period will cause a series of problems like pore throat blocking, surfactant and polymer are not preferable for such formation when compared with gel. Thus, the gel is selected as the ideal fracture fluid for well A, and the surfactant is the optimum fracture fluid for well B similarly. Figure 5 shows the 2D slices of core samples at various gel-soaking stages for well A.

As shown in Fig. 5, the pores show a little shrinkage in the 1st day and amplify gradually in the next few days. The clay minerals of the samples swell initially and lead to the porosity decrease. Then, the calcite is dissolved slightly after which leads to the porosity increase. Figure 6 shows the 2D slices of core samples at various surfactant soaking times for well B.

For the well A using gel as the optimized fracture fluid, the porosity shows 23.02% decrease during the first day. Since there are 13.6% clay mineral, clay swelling is the dominant mechanism for porosity decrease in this stage. Then, the porosity increases gradually resulting from the calcite dissolution which surpass the clay swelling later. However, the porosity does not recover to the original level after 15-day's soaking. That is to say, the optimized gel fracture fluid would still cause 10.44% porosity decrease after 15-day's well A shut-in. For the well B with the surfactant as the optimized fracture fluid, the porosity shows 35.89% decrease during the first three days. Because the clay mineral content (22.6%) in well B is higher than that in well A (13.6%), the porosity decrease is much sharper.

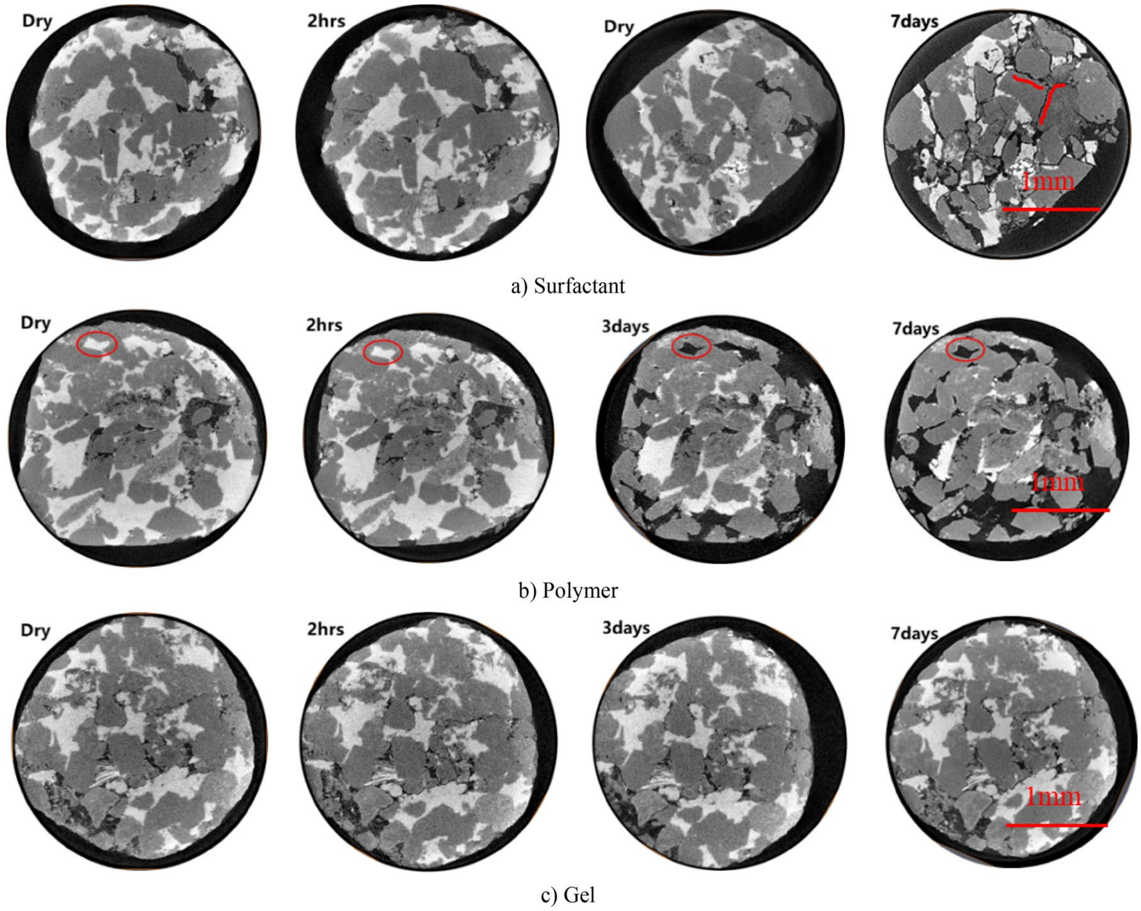

Fig. 3 Gray images of core samples (Well A) soaking in different fracture fluids for different durations

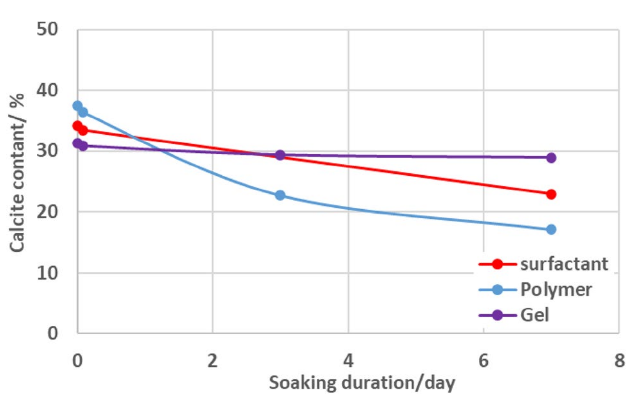

Fig. 4 Calcite variation after different fluids soaking durations (Well A)

After, the porosity also increases gradually due to calcite dissolution. The porosity decreases by 13.17% in total after 15-day's well B shut-in.

Porosity variation, defined as the ratio of the current porosity to the initial porosity of dry sample, is calculated to quantify the pore structure alteration at various times. Figure 7 shows the porosity variation for the optimized fracture fluid, the gel used in well A and surfactant used in well B.

Well shut-in optimization

In order to optimize the shut-in time, oil displacing water process (namely, flow back production process) is simulated using LBM with the 3D structure data of different soaking durations to evaluate the residual oil saturations. Initially, the digital samples are fully water saturated. Figure 8 shows the simulated residual oil distribution at various shut-in times, based on the CT images for well A using gel. Figure 9 compares the simulated residual oil saturation for the gel in well A and surfactant in well B, respectively.

The dry core sample has the highest residual oil saturation, followed by the one after 1-day soaking in gel. The one after 3-day soaking in surfactant have the lowest residual oil saturation. This outcome is complied with Fig. 7. Porosity decrease resulting from clay swelling will lead to residual oil saturate decrease after well shut-in.

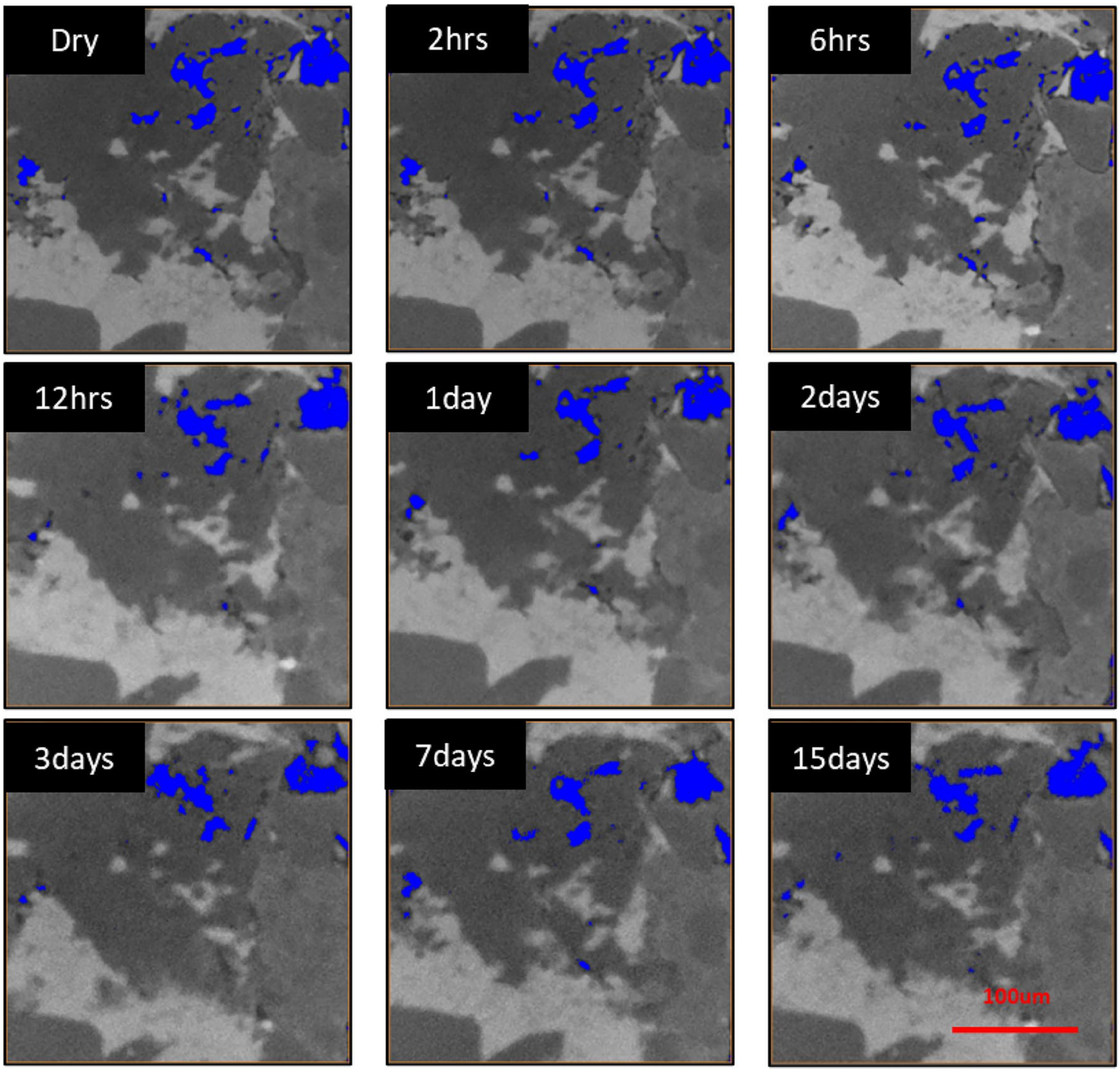

Fig. 5 2D slices of core samples at various gel soaking intervals for Well A (Blue denotes pore, and gray denotes rock skeleton)

After, porosity increase resulting from calcite dissolution will lead to residual oil saturation increase. For the well A using gel, the porosity decreases by 23.04% in 1-day after shut-in, which leads to 40.37% decrease for the residual oil saturation. The porosity increases by 12.58% later which leads to 26.46% increase for the residual oil saturation. After 15-day shut-in, the residual oil saturation reduces by 24.60% in total, and the porosity reduces by 10.53%. Thus, 6 h is recommended for the shut-in time in well A. For the well B using surfactant, the porosity decreases by 35.89% in the first 3-days after shut-in, which leads to 44.91% decrease in the residual oil saturation. The porosity increases by 35.44% later which leads to 29.43% increase for the residual oil saturation. After 15-day shut-in, the oil saturation reduces by 28.69% in total and the porosity reduces by 13.17%. Similarly, 1 day is recommended for the shut-in time in well B.

Conclusions

In this study, digital rock technology is combined with the laboratory fracture fluids soaking experiments to evaluate the formation damages for tight sandstone reservoir. Fracture fluid is optimized by comparing the CT images of core samples soaking in different types of fracture fluids at various time intervals. The flowback process is simulated by LBM to obtain the residual oil saturation, and the optimum well shut-in time is recommended. This method of fracture fluids and well shut-in time optimization will provide fundamentals to guide the selection of the fracture fluids and

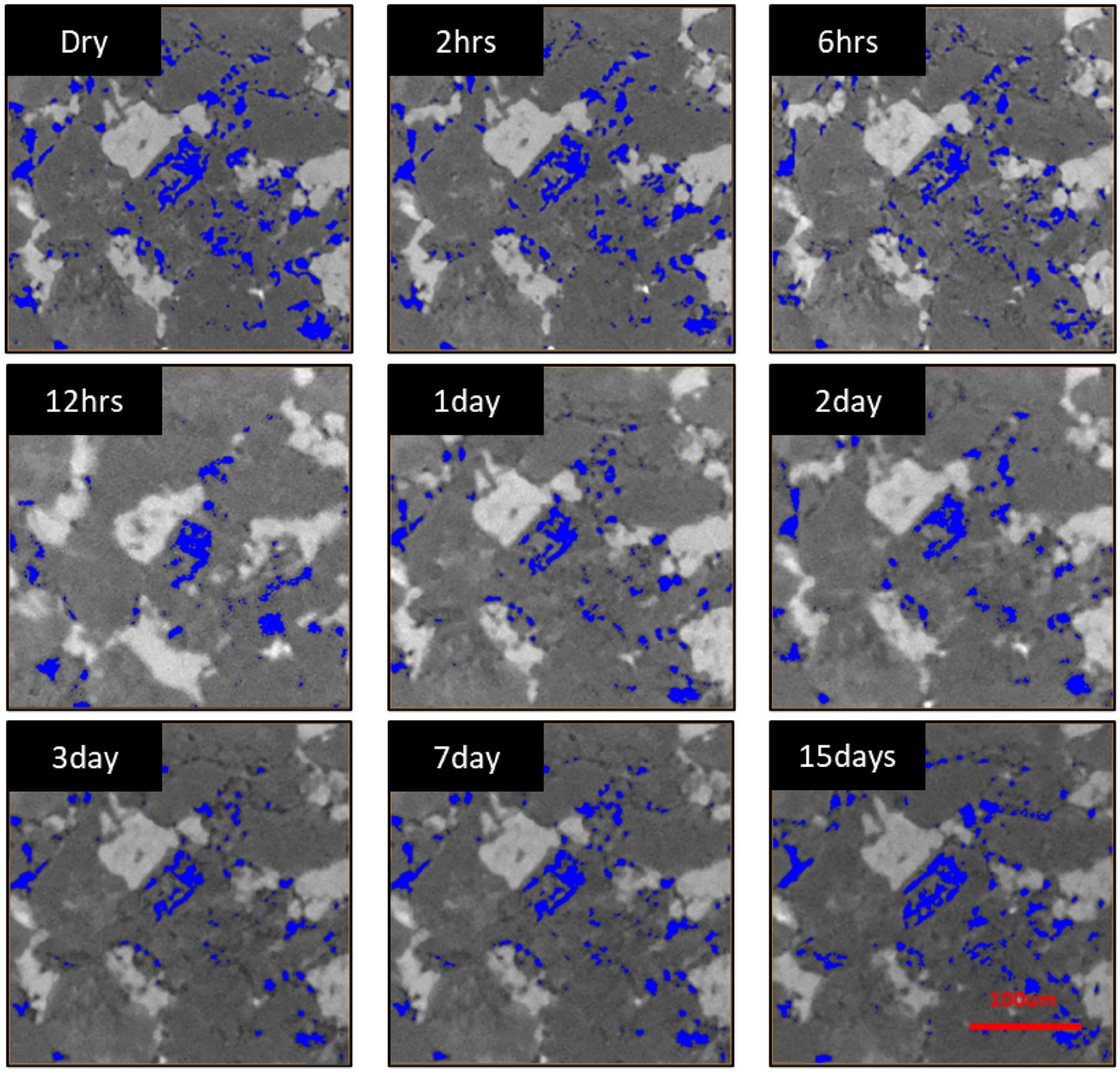

Fig. 6 2D slices of core samples at various surfactant soaking intervals for Well B (Blue denotes pore, and gray denotes rock skeleton)

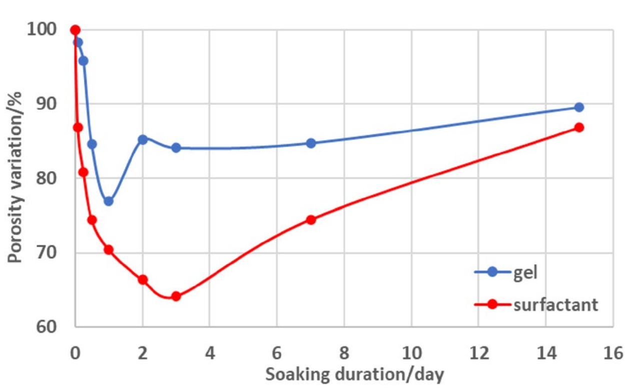

Fig. 7 Porosity variation after different fluids soaking durations

onsite fracturing operation. This in situ technology can also be used to optimize the EOR operations, such as quantification of wettability for surfactant or low salinity waterflood, variation of pore structure for polymer or bright waterflood (Tadesse et al. 2016; Frampton et al. 2004). Based on the results, we can conclude that:

(1) From CT images and porosity calculation, the well shut-in process can cause irreversible damage to tight sandstone reservoir even for the most preferred fracture fluid. In the initial shut-in stages, clays swelling dominates the pore structure alternation and causes the porosity decrease. After, calcite dissolution will lead to slight porosity recovery as shown in Figs. 4 and 7. This phenomenon can be clearly observed by comparing the

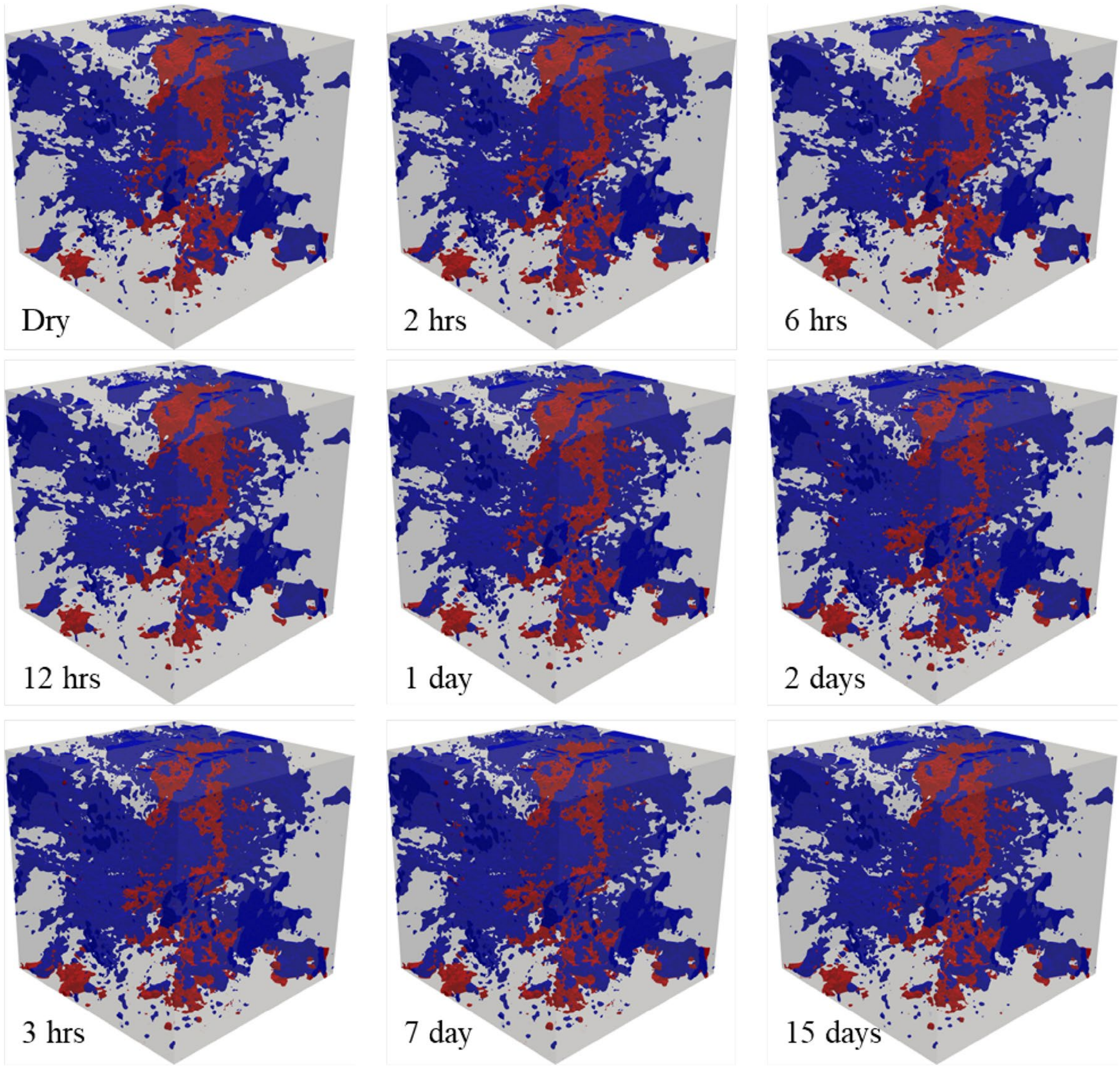

Fig. 8 Fluid distributions for simulations of water displacing oil (Blue denotes water, and red denotes oil)

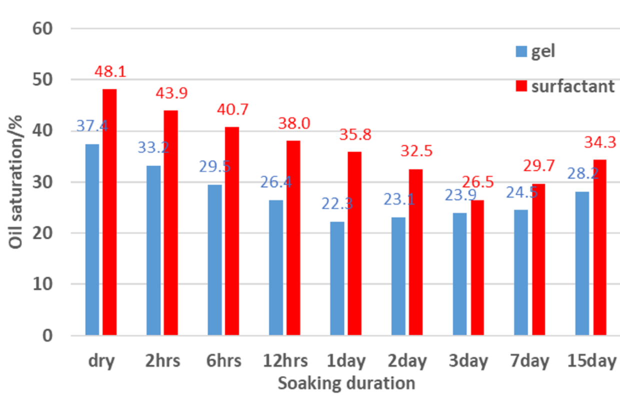

Fig. 9 Residual oil saturations after different soaking durations

CT images before and after the experiments at various soaking times.

(2) We simulated the two-phase flow based on the CT images at various soaking times to mimic the flowback process after well shut-in. The simulated residual oil saturation will decrease first and then increase after, which is mainly due to the porosity change caused by clay swelling initially and calcite dissolution after.

(3) Since the 3D pore structure in different well shut-in periods does not take the dispersion or dissolution of the clay particles into consideration, the actual oil saturation in flowback process will probably be much lower due to the mineral dispersion, transportation, and deposition. A further study of the sediment's transportation is recommended.

Acknowledgments This work was supported by the Program for Guangdong Introducing Innovative and Entrepreneurial Teams (No. 2017ZT07G264); Shenzhen Peacock Plan (No. KQTD2017033114582189) and The Shenzhen Science and Technology Innovation Committee (JCYJ20170817152743178)

References

Andrew M, Bijeljic B, Blunt M (2014) Pore-by-pore capillary pressure measurements using x-ray micro tomography at reservoir conditions: curvature, snapoff, and remobilization of residual CO_2. Water Resour Res 50(11):8760–8774. https://doi.org/10.1002/2014WR015970

Arganda-Carreras I, Kaynig V, Rueden C et al (2017) Trainable Weka segmentation: a machine learning tool for microscopy pixel classification. Bioinformatics 33(15):2424–2426

Bing W, Li Q, Wang Y et al. (2018) An experimental study of enhanced oil recovery EOR using a green nano-suspension. SPE-190283-MS. https://doi.org/10.2118/190283-MS.

Blunt MJ, Bijeljic B, Hu D et al (2012) Pore-scale imaging and modeling. Adv Water Resour 51:197–216. https://doi.org/10.1016/j.advwatres.2012.03.003

Cancelliere A, Chang C, Foti E et al (1990) The permeability of a random medium: comparison of simulation with theory. Phys Fluids 2(12):2085–2088. https://doi.org/10.1063/1.857793

Cense A W, Berg S, Jansen E (2011). Direct visualization of designer water flooding in model experiments. SPE-144936-MS. https://doi.org/10.2118/144936-MS.

Frampton H, Morgan J C, Cheung S K, Munson L, Chang K T, Williams D (2004) Development of a novel waterflood conformance control system. In: Paper presented at the SPE/DOE Symposium on Improved Oil Recovery, Tulsa, Oklahoma. https://doi.org/10.2118/89391-MS.

Fredrich J T (2014) Digital rocks: developing an emerging technology through to a proven capability deployed in the business. Amsterdam, Society of Petroleum Engineers. https://doi.org/10.2118/170752-MS.

Guo C, Wang X, Wang H et al (2018) Effect of pore structure on displacement efficiency and oil-cluster morphology by using micro computed tomography (μCT) technique. Fuel 230:430–439. https://doi.org/10.1016/j.fuel.2018.11.124

Izgec O (2009) Reactive flow in vuggy carbonates: methods and models applied to matrix acidizing of carbonates. Texas A&M University, Texas.

Jerauld G R (2017) Validation of a workflow for digitally measuring relative permeability. Soc Petrol Eng. https://doi.org/10.2118/188688-MS.

Kang Q, Zhang D, Chen S (2002) Displacement of a two-dimensional immiscible droplet in a channel. Phys Fluids 14(9):3203–3214

Li Z, Lu T, Lei T (2011) CO_2 and viscosity breaker assisted steam huff and puff technology for horizontal wells in a super-heavy oil reservoir. Pet Explor Dev 38(5):600–605

Liang T, Longoria RA, Lu J (2017) Enhancing hydrocarbon permeability after hydraulic fracturing: laboratory evaluations of shut-ins and surfactant additives. SPE J 22(04):1–11

Martys NS, Chen H (1996) Simulation of multicomponent fluids in complex three dimensional geometries by the lattice Boltzmann method. Phys Rev E 53(1):743–750. https://doi.org/10.1103/PhysRevE.53.743

Mclendon W, Koronaios P, Enick R et al (2014) Assessment of CO2-soluble non-ionic surfactants for mobility reduction using mobility measurements and CT imaging. J Pet Sci Eng 119(3):196–209. https://doi.org/10.1016/j.petrol.2014.05.010

Mcphee C, Reed J, Zubizarreta I (2015) Core analysis: a best practice guide. Elsevier, Amsterdam

Mukherjee PS-K (2016) Digital rock analysis—providing SCAL properties for the matrix of tight carbonates of the Najmah-Sargelu formation, Kuwait. Soc Petrol Eng. https://doi.org/10.2118/182864-MS

Nasiru SM, Bashirul H, Dhafer A et al (2020) Comparative study of green and synthetic polymers for enhanced oil recovery. Polymers 12(10):2429. https://doi.org/10.3390/polym12102429

Pan C, Hilpert M, Miller CT (2004) Lattice-Boltzmann simulation of two phase flow in porous media. Water Resour Res 40(1):62–74

Rassenfoss S (2011) Digital rocks out to become a core technology. J Petrol Technol 63(05):36–41. https://doi.org/10.2118/0511-0036-JPT

Rui Z, Cui K, Wang X (2018) A quantitative framework for evaluating unconventional well development. J Pet Sci Eng 166:900–905

Shan X, Doolen G (1995) Multi-component lattice-Boltzmann model with interparticle interaction. J Stat Phys 81(1–2):379–393

Singh K, Niven R, Senden T et al (2011) Remobilization of residual non-aqueous phase liquid in porous media by freeze-thaw cycles. Environ Sci Technol 45(8):3473–3478. https://doi.org/10.1021/es200151g

Sun H, Vega S, Tao G (2017) Analysis of heterogeneity and permeability anisotropy in carbonate rock samples using digital rock physics. J Pet Sci Eng 156:419–429. https://doi.org/10.1016/j.petrol.2017.06.002

Sun H, Belhaj H, Tao G (2019) Rock properties evaluation for carbonate reservoir characterization with multi-scale digital rock images. J Pet Sci Eng 175:654–664. https://doi.org/10.1016/j.petrol.2018.12.075

Tadesse W T, Waleed A, Ramona M G, Hossein K, Ali M A (2016) Low-salinity water-alternating-CO2 EOR. J Petrol Sci Eng 42:101–118. https://doi.org/10.1016/j.petrol.2016.01.031.

Vocke C P (2018) Estimation of petrophysical properties of tight rocks from drill cuttings using image analysis: an integrated laboratory based approach. In: SPE Canada Unconventional Resources Conference. Calgary, Alberta, Canada: Society of Petroleum Engineers.

Walls JD (2012) Shale reservoir properties from digital rock physics. Soc Petrol Eng. https://doi.org/10.2118/152752-MS

Wang S, Tokunaga TK, Wan J (2016) Capillary pressure-saturation relations in quartz and carbonate sands: limitations for correlating capillary and wettability influences on air, oil, and supercritical CO_2 trapping. Water Resour Res 52(8):6671–6690. https://doi.org/10.1002/2016wr018816

Wang X, Xiao P, Yang Z (2020) Laboratory and field-scale parameter optimization of CO_2 huff-n-puff with the staged-fracturing horizontal well in tight oil reservoirs. J Petrol Sci Eng. https://doi.org/10.1016/j.petrol.2019.106703

Xie J, He S, Zu Y, Lamy-Chappuis B (2017) Relative permeabilities of supercritical CO_2 and brine in carbon sequestration by a two-phase lattice Boltzmann method. Heat Mass Tran 53(8):2637–2649. https://doi.org/10.1007/s00231-017-2007-6

Yang J, Dai X, Xu Q (2021a) Lattice Boltzmann modeling of interfacial mass transfer in a multiphase system. Phys Rev E 104(1):15307. https://doi.org/10.1029/2003wr002120

Yang J, Dai X, Xu Q (2021b) Pore-scale study of multicomponent multiphase heat and mass transfer mechanism during methane hydrate dissociation process. Chem Eng J 423:130206. https://doi.org/10.1016/j.cej.2021.130206

You L, Xie B, Yang J (2019) Mechanism of fracture damage induced by fracturing fluid flowback in shale gas reservoirs. Natural Gas Industry B 6:366–373. https://doi.org/10.1016/j.ngib.2018.12.005

Zhao X, Blunt M, Yao J (2010) Pore-scale modeling: effects of wettability on waterflood oil recovery. J Pet Sci Eng 71(3–4):169–178. https://doi.org/10.1016/j.petrol.2010.01.011